

**Kinetically induced ordering oscillation during epitaxial growth of a fcc multilayer alloy**

Lin Shi and Jun Ni

*Department of Physics, Tsinghua University, Beijing 100084, People's Republic of China*

(Received 11 August 2003; revised manuscript received 20 January 2004; published 28 April 2004)

The kinetics of ordering in fcc multilayer alloys during the epitaxial growth is investigated by the kinetic mean-field method. The kinetic phase diagrams for the epitaxial alloy of a fcc multilayer are calculated. We have found that there is a kinetically induced oscillatory ordered phase in addition to the equilibrium ordered phase in the kinetic phase diagrams. This ordering oscillation is caused by the kinetic correlation of different growth processes. It occurs with growth condition of higher deposition rate and in materials with high jumping barrier energies.

DOI: 10.1103/PhysRevB.69.155428

PACS number(s): 81.15.Aa, 64.60.Cn, 64.60.My, 82.40.Bj

**I. INTRODUCTION**

Epitaxial growth has been used to prepare materials in a nonequilibrium state or with artificial structure for the purpose of fabricating high-quality low-dimensional structures with novel physical properties. Much attention has been devoted to the growth of ordering structures in epitaxial alloys and various metastable ordered phases have been obtained using epitaxial growth process.<sup>1-12</sup> The epitaxial ordered structures in  $\text{Si}_x\text{Ge}_{1-x}$  alloy,<sup>1-4</sup> III-V semiconductor alloys,<sup>5-8</sup> and in some metal alloys<sup>9-12</sup> are thermodynamically unstable in the bulk. The ordering in these alloys is established in the growth layer during the epitaxial growth and is then frozen-in as growth proceeds. Theoretically, the growth of an alloy with short-range order is studied using the kinetic mean-field model.<sup>13</sup> The interplay between compositional ordering and surface roughening during the epitaxial growth of a binary alloy is investigated using the kinetic mean field<sup>14</sup> and the Monte Carlo method.<sup>15-17</sup> The Monte Carlo method has also been used to simulate the kinetics of ordering in III-V semiconductor alloys during epitaxial growth due to step flow<sup>18</sup> and organometallic vapor-phase epitaxial growth of ordered films.<sup>19</sup> The epitaxial growth of alloys is a nonequilibrium process controlled by various relaxation processes such as the surface diffusion, adsorption, and evaporation. The amount of long-range order and its presence depend sensitively on the growth condition. Comprehending the ordering process during the epitaxial growth is important, but much remains unknown, especially about the kinetic phase diagrams which present the global status of ordering in the epitaxial growth of alloys.

In this paper, we have made a study on the global feature, described by the kinetic phase diagrams, of ordering in the epitaxial growth of an fcc multilayer alloy. In particular, we have found a kinetically induced ordering oscillation. The occurrence of this ordering phenomenon is attributed to the kinetic correlation of different growth processes.

**II. METHODS**

We consider the epitaxial growth of an fcc multilayer alloy in (001) direction. The system consists of three components, two species ( $A$  and  $B$ ) of atoms in alloy and vacancy ( $C$ ) on the growth layer. The system is described by the

stochastic lattice gas model with the Hamiltonian

$$\mathcal{H} = \sum_{ij} \sum_{ss'} E_{ij}(\mathbf{r}_s - \mathbf{r}_{s'}) c_i^s c_j^{s'} \quad (1)$$

The variable  $c_i^s = 1$  if the site  $s$  is occupied by the  $i$  ( $=A, B, V$ ) species and is zero otherwise. The notation  $ss'$  means the summation over the pairs of neighboring lattice sites.  $E_{ij}(\mathbf{r}_s - \mathbf{r}_{s'})$  represents the interaction energy between the  $i$  species at  $\mathbf{r}_s$  and the  $j$  species at  $\mathbf{r}_{s'}$ .

The lattice of planes in (001) direction of an fcc alloy is square lattice. To describe the ordering of the system with the nearest- and the next-nearest-neighbor interactions, we divide the square lattice of each layer into two sublattices. The interaction between an  $i$  atom and a  $j$  atom, which is the nearest neighbor of the  $i$  atom in the first underlayer, is the nearest-neighbor interaction and the interaction between an  $i$  atom and a  $k$  atom, which is the nearest neighbor of the  $i$  atom in the second underlayer, is the next-nearest-neighbor interaction. In many materials such as CuAu alloy, the third-nearest-neighbor interaction has less effect on the structure of the material.<sup>20</sup> In this work we only consider the nearest- and the next-nearest-neighbor interactions. In the kinetic mean-field approximation,<sup>21,22</sup> the configurations of the system are described by the site probabilities.  $P_i^s(m, t)$  is the probability occupied by  $i$  ( $=A, B, V$ ) species in  $s$  ( $=\alpha, \beta$ ) sublattices on the  $m$ th growth layer at time  $t$ . In the calculation, the site probabilities satisfy the normalization conditions:

$$\sum_{i(A,B,V)} P_i^\alpha(m, t) = 1, \quad \sum_{i(A,B,V)} P_i^\beta(m, t) = 1. \quad (2)$$

The growth process comprises the three relaxation processes: the surface diffusion, adsorption, and evaporation processes. We use the micromaster equation method<sup>22,23</sup> to describe the atomic diffusion process. The cluster activation method<sup>23</sup> is used for the treatment of the micromaster equation. We assume that the atomic distributions in the subsurface layer are fixed when a new layer is formed due to the very low bulk diffusion coefficients at the growth temperature and only surface diffusion in which an  $A$  or  $B$  atom jumps to an empty nearest-neighbor adsorption site is considered. We use the basic exchange probability function  $Y_{ij}(m, t)$  to represent the

exchange probability between species  $i$  and species  $j$  (one of them is a vacancy  $V$ ) on the  $m$ th layer at time  $t$  per unit time. The activation energy for the atomic jumping consists of the symmetric activation contribution and the antisymmetric activation contribution.<sup>23</sup> The symmetric activation contribution is independent of the local atomic arrangement, which corresponds to the average barrier energy  $U_i$  for the exchange between atom  $i$  and vacancy. The antisymmetric activation contribution depends on the local atomic arrangement, which corresponds to the energy difference for the atom-vacancy interchange. Each basic atom-vacancy exchange is affected by the interactions with the species on the neighboring sites. There is a factor  $\exp(-\Delta E_{ij}/2k_B T)$  due to the influence of the neighboring species on the exchange species which leads to a bond broken factor  $W_{ij}$  (Refs. 22 and 23) describing the effects of the neighboring sites.  $\Delta E_{ij}$  is the energy difference for the atom-vacancy interchange.  $Y_{ij}(m)$  is proportional to the characteristic exchange rate  $\nu_{ij}$ , the barrier energy factor  $\exp(-U_i/k_B T)$ , the site probabilities  $P_i^\alpha$  and  $P_j^\beta$ , and the bond broken factor for the atom-vacancy exchange  $W_{ij}$  describing the effects of the neighboring sites. Because one of  $ij$  is an atom, the exchange rate is inversely proportional to the probability that the supporting sites are not occupied by vacancy in the underlayer.

We use the solid on solid (SOS) restriction condition<sup>24</sup> in the growth process. The atoms are supported by the atoms in the underlayer in the growth process. We define  $X_i^s(m, t)$  as the adsorption probability per unit time of the species  $i$  on the sublattice  $s$  on the  $m$ th layer at time  $t$ . Under the SOS restriction condition, an atom can adsorb when the supporting sites are not vacancies.  $X_i^s$  is proportional to the characteristic adsorption rate  $w_i$ , the vacancy probability  $P_i^s$  and a factor describing the SOS restriction. We define  $Z_i^s(m, t)$  as the evaporation probability per unit time of the species  $i$  from the  $s$  sublattice on the  $m$ th layer at time  $t$ . Under the SOS restriction condition, an atom can only evaporate when the sites over it are vacancies.  $Z_i^s(m, t)$  is proportional to the characteristic evaporation rate  $w'$ , the site probability  $P_i^s$  of the evaporation atom, the chemical potential factor  $\exp(-\mu_i/k_B T)$  ( $\mu_i$  is the chemical potential of the  $i$  species), the bond broken factor for the evaporation  $V_i^s$ , and a factor describing the SOS restriction. The characteristic adsorption rate can be related to the characteristic evaporation rate due to the detailed balance condition between the evaporation and the adsorption.<sup>21</sup>

The kinetics of growth is described by the following differential equations with all the three contributions from the atom-vacancy exchange, evaporation, and adsorption processes:

$$\begin{aligned} \frac{dP_i^\alpha(m)}{dt} &= 4[Y_{Vi}(m) - Y_{iV}(m)] + Z_i^\alpha(m) + X_i^\alpha(m), \\ \frac{dP_i^\beta(m)}{dt} &= 4[Y_{iV}(m) - Y_{Vi}(m)] + Z_i^\beta(m) + X_i^\beta(m). \end{aligned} \quad (3)$$

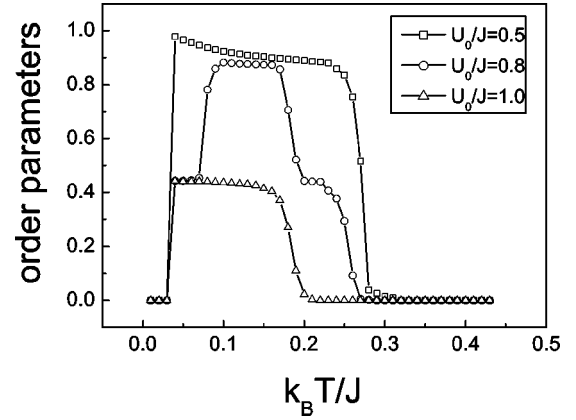


FIG. 1. The average order parameters as a function of temperature with  $w/\nu = 5 \times 10^{-3}$  and  $\mu_A = \mu_B = 0.025$  eV.

The atomic configurations are determined by the occupation probability  $P_i^s$ . The symmetry of the phase structures is described by the following order parameters in each layer related to the site probability  $P_i^s$ ,

$$\gamma_A(m) = P_A^\alpha(m) - P_A^\beta(m), \quad \gamma_B(m) = P_B^\alpha(m) - P_B^\beta(m). \quad (4)$$

When the layers are filled fully,  $\gamma_B(m) = -\gamma_A(m)$  because of the site probabilities' normalization conditions. The concentrations are related to the site probability  $P_i^s$  as follows:  $x_i(m) = [P_i^\alpha(m) + P_i^\beta(m)]/2$ . The coverage  $\theta$  of the layers is the sum of the concentration of the atomic species. The differential equations are solved numerically by the Runge-Kutta method. Initially the growth layer is empty. The growth process is described by the evolution of the concentrations and the order parameters governed by the above differential equations.

### III. RESULTS

In the epitaxial growth process of an ordered alloy, the phase formed during the growth process becomes disordered due to the entropy effect at high temperature, while at very low temperature, there is kinetic frozen-in due to the low atomic exchange rates and a metastable disordered phase is formed during the growth process. The ordered phase only forms at suitable temperature. The ordered phase formed during the growth process generally has the same structure as the equilibrium ordered phase. Figure 1 shows the structure parameters of a typical ordering case as a function of growth temperature. In this typical case, the growth of 32 layers is calculated, and the nearest-neighbor interaction energies are taken as  $E_{AB}^{(1)} = -0.05$  eV,  $E_{AA}^{(1)} = E_{BB}^{(1)} = 0.0$  eV,  $E_{AV}^{(1)} = E_{BV}^{(1)} = E_{VV}^{(1)} = 0.0$  eV and the next-nearest-neighbor interaction energies are taken as zero. The effect of the next-nearest-neighbor interaction will be discussed later. First, we take  $U_A = U_B$  and denote  $U_0 \equiv U_A = U_B$ . We also take the atomic exchange rates  $\nu_{AV} = \nu_{BV}$  and denote  $\tau_D = \nu_D^{-1} \equiv \nu_{AV}^{-1}$ . The difference between atomic energy and dynamic parameters for A and B atoms may result in transient ordered states,<sup>22,25</sup> which will be discussed later. The system with such energy

parameters is expected to exhibit ordering. The interaction energy  $E_{ij}$  affects the equilibrium phase transition of the system only through the interchange energy  $J = -2E_{AB}^{(1)} + E_{AA}^{(1)} + E_{BB}^{(1)}$ . When  $J > 0$ , the system forms an ordering phase, and when  $J < 0$ , the system forms a segregable phase. In our case,  $J = 0.1 \text{ eV} > 0$  and the system exhibits an ordering phase. In our paper, the value of energy parameters is normalized with  $J$ . The kinetic processes are also controlled by the barrier energy  $U_0$ . When the layers are filled fully,  $|\gamma_A| = |\gamma_B|$  and the ordered parameter in Fig. 1 is for both  $\gamma_A$  and  $\gamma_B$ . When  $U_0/J = 0.5$ , as shown in Fig. 1, the system is in disordered phase at high temperature ( $k_B T/J > 0.27$ ) and in ordered phase at moderate temperature ( $0.04 < k_B T/J < 0.27$ ). When the temperature is very low ( $k_B T/J < 0.04$ ), it is again in disordered phase. In addition to this normal ordering during growth process, we find a phenomenon of kinetically induced ordering oscillation in the epitaxial multilayer structure. As shown in Fig. 1, when  $U_0/J = 0.8$ , there are two more steps in the curve of the average order parameter. The kinetically induced ordering oscillation occurs at the temperature region where the average order parameter is about 0.5. The step where the average order parameter is about 1 corresponds to the equilibrium ordered phase. In this kinetically induced oscillatory ordered phase, as shown in Fig. 2(a), the odd layers are disordered where the order parameter is zero and the even layers are ordered where the order parameter is about 1. When we average the order parameter of all layers, the average order parameter is about 0.5 for the kinetically induced oscillatory ordered phase. Because our calculations are on the growth of 32 layers, the 32nd layer is the last layer and is always the surface layer. Thus the order parameter of the 32nd layer is larger than that of other layers. In the average of order parameter, we did not include this special layer. When  $U_0/J = 1.0$ , only the kinetically induced oscillatory ordered phase occurs and the average order parameter is about 0.5 for the ordered phase.

Since we consider only surface diffusion, the atoms in the underlayer are considered to be frozen in the growth process. The order-disorder phase transition temperature for very small  $\kappa = \omega/\nu$  should be close to that in the square lattice. The order-disorder phase transition temperature is  $k_B T/J = 0.54$  with  $U_0 = 0.5$  and  $\omega/\nu = 5 \times 10^{-4}$ , which is close to the phase-transition temperature of the square lattice  $k_B T/J = 0.55$ .<sup>26</sup> Since the growth process is a nonequilibrium process, the phase-transition temperature is affected by the barrier energy. The barrier energy factor  $\exp(-U_{ij}/k_B T)$  is decreased with the increase of the barrier energy. Thus the exchange probability which is proportional to the barrier energy factor decreases and induces the phase-transition temperature to decrease, as shown in Fig. 1.

### A. The kinetic phase diagram

The growth parameters have significant effects on the phase structure formed during the growth process. There are phases which have no corresponding phase in the equilibrium phase diagram. They are formed only kinetically in a suitable growth condition. If we take the characteristic rate

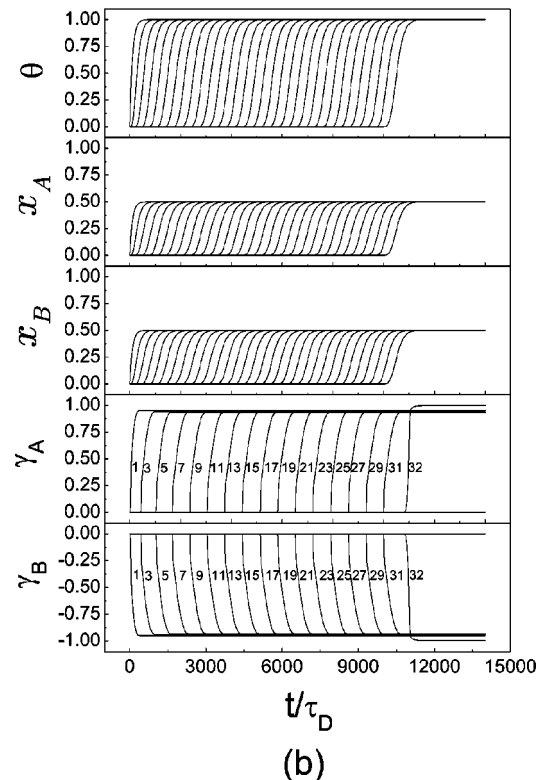
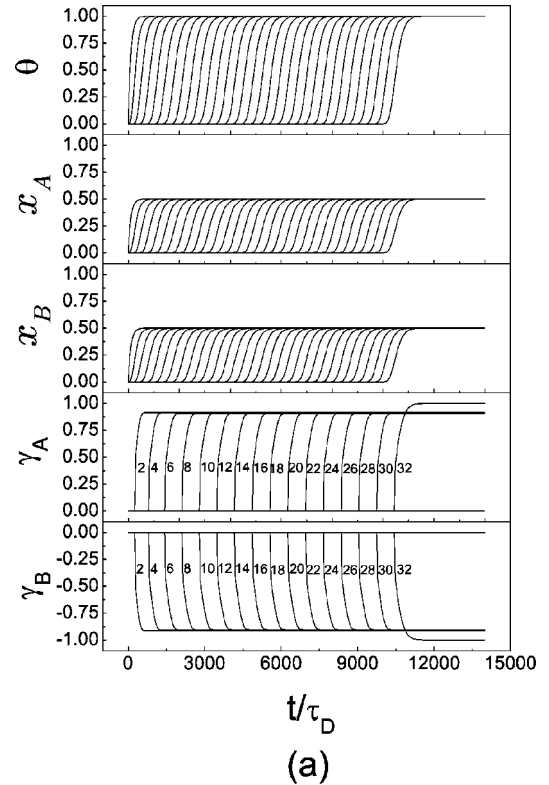


FIG. 2. The evolution of the coverage  $\theta$ ; the concentrations  $x_A, x_B$ ; and the order parameters  $\gamma_A, \gamma_B$  during the growth process for the kinetically induced oscillated ordering at the temperature  $k_B T/J = 0.06$  with  $\kappa = 5 \times 10^{-3}$ ,  $U_0/J = 0.8$ , and  $\mu_A = \mu_B = 0.025 \text{ eV}$ . (a) For substrate with  $P_A^\alpha = P_B^\alpha = 1$  and (b) for substrate with  $P_A^\alpha = P_B^\alpha = 0.5$ .

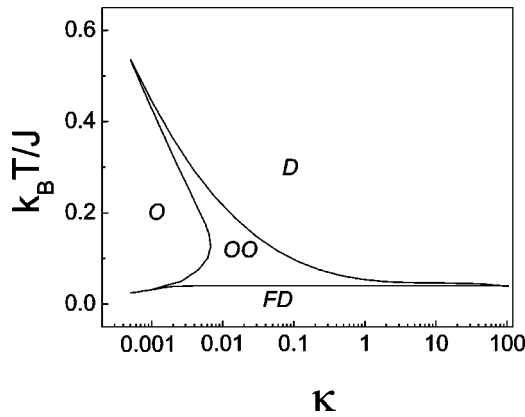


FIG. 3. The kinetic phase diagram with temperature and the ratio  $\kappa$  as parameters with  $U_0/J=1.0$  and  $\mu_A=\mu_B=0.025$  eV.

and the barrier energy as phase diagram parameters, we can draw the kinetic phase diagrams shown in Figs. 3 and 4. From the kinetic phase diagrams, we can obtain the formation conditions for various phases formed during the kinetic growth. Figure 3 shows the phase diagrams with the temperature and the ratio  $\kappa=\omega/\nu$  between the characteristic adsorption rate and exchange rate as parameters. In the figures, the phase  $O$  denotes the equilibrium ordered phase, the phase  $D$  denotes the disordered phase, the phase  $OO$  denotes the kinetically induced oscillatory ordered phase, and the phase  $FD$  is the frozen-in disordered phase. When the characteristic exchange rate is large ( $\kappa$  is small), the atomic migrations are fast during the growth process and it is easy for atoms to reach the equilibrium and form an ordered phase. When the characteristic adsorption rate is large ( $\kappa$  is large), the growth surface is covered with atoms quickly and the atoms in the underlayer hardly have a chance to migrate, then only the disordered phase is formed. The ordered phase is formed only for a small characteristic adsorption rate. As shown in Fig. 3, the growth phase is the frozen-in disordered phase at low temperature and is the entropy induced disordered phase at high temperature. When the ratio  $\kappa$  between the characteristic atomic adsorption rate and exchange rate is small, the system is close to the equilibrium state, the growth phase is

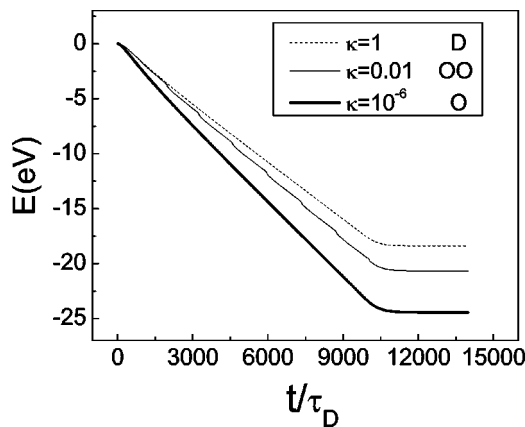


FIG. 4. The evolution of energy of the system with different  $\kappa$ ,  $k_B T/J=0.1$ ,  $U_0/J=1.0$ , and  $\mu_A=\mu_B=0.025$  eV.

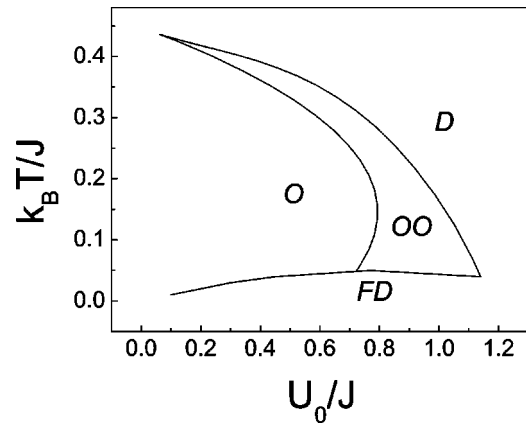


FIG. 5. The kinetic phase diagram with temperature and the barrier energy as parameters with  $\kappa=5 \times 10^{-3}$  and  $\mu_A=\mu_B=0.025$  eV.

the equilibrium ordered phase at suitable temperature. When  $\kappa$  is large, the growth phase is kinetically induced oscillatory ordered phase. It should be noted that in the kinetic phase diagram of Fig. 3, there is a reentrant transition between phases  $O$  and  $OO$ . Both at lower and higher temperatures, the  $OO$  phase occurs due to the kinetic effect. The boundary line between the  $D$  and  $OO$  phases approaches the line between the  $FD$  and  $OO$  phases with the increase of  $\kappa$  because the system is more disordered for larger ratio  $\kappa$  and then they are annexed, at a point we call kinetic critical point, following the critical point between the vapor phase and liquid phase. We have calculated the evolution of the energy  $E$  of the system with different  $\kappa$  as shown in Fig. 4. The smaller  $\kappa$  leads to a phase closer to equilibrium. The energy of the oscillatory ordered phase ( $\kappa=0.01$ ) is larger than that of the ordered phase ( $\kappa=10^{-6}$ ) and smaller than that of the disordered phase ( $\kappa=1$ ). The curve for the ordered phase ( $\kappa=10^{-6}$ ) in Fig. 4 is the evolution of the energy of the equilibrium phase approximately since  $\kappa$  is very small. This means that the phases closer to equilibrium have smaller energy. Figure 5 is the phase diagram with temperature and the barrier energy as parameters. The barrier energy affects the atomic diffusion rate in the growth layer. The lower the barrier energy is, the larger the atomic diffusion rate is and the easier the equilibrium ordered structure forms. As shown in

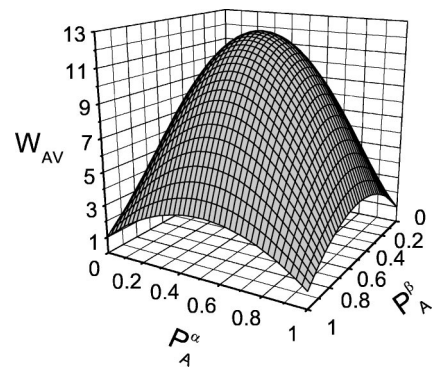


FIG. 6. The relation between the bond broken factor  $W_{AV}$  for atom  $A$  and vacancy exchange with the structure of the underlayer.

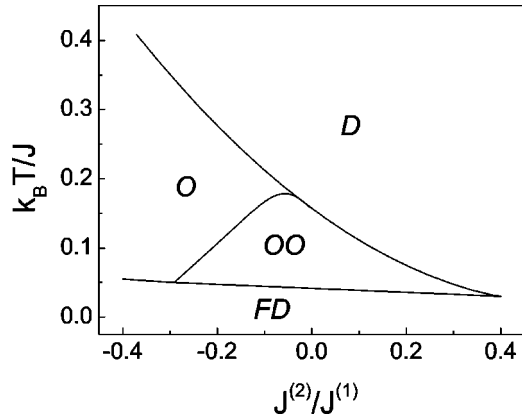


FIG. 7. The kinetic phase diagram with temperature and the next-nearest-neighbor interaction as parameters with  $E_{AB}^{(1)} = -0.05$  eV,  $U_0/J = 1.0$ ,  $\kappa = 5 \times 10^{-3}$ , and  $\mu_A = \mu_B = 0.025$  eV.

Fig. 5, the maximum of the barrier energy for the occurrence of the oscillatory ordered phase is 1.14 with  $\kappa = 5 \times 10^{-3}$ . The characteristic exchange rate  $\mu_D$  and the barrier energy affect the growth of the system by the factor  $\mu_D \exp(-U_0/k_B T)$ . The maximum of the barrier energy for the oc-

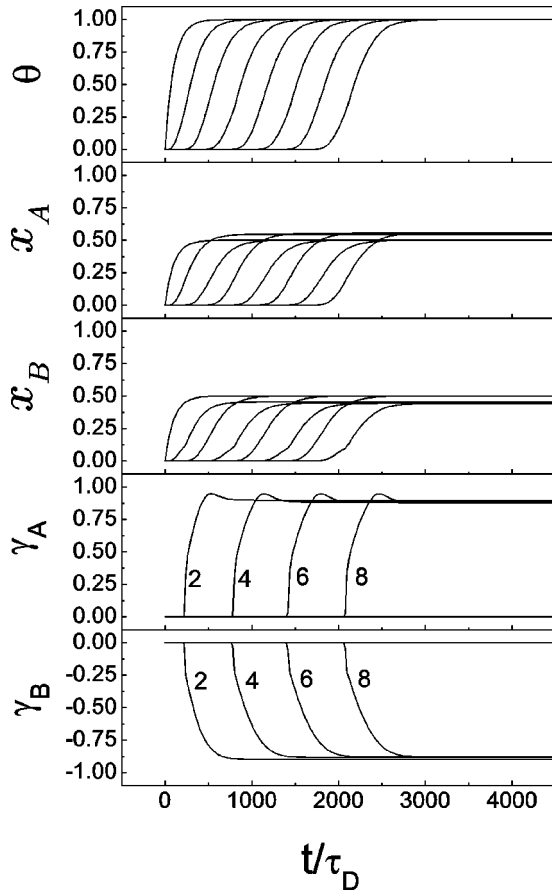


FIG. 8. The evolution of the coverage, the concentrations, and the order parameters during the growth process with  $E_{AA}^{(1)} = 0.001$  eV,  $E_{BB}^{(1)} = 0.01$  eV,  $E_{AB}^{(1)} = -0.05$  eV,  $k_B T/J = 0.07$ ,  $U_0/J = 1.0$ ,  $\kappa = 5 \times 10^{-3}$ ,  $\mu_A = \mu_B = 0.025$  eV, and substrate with  $P_A^\alpha = P_A^\beta = 1$ .

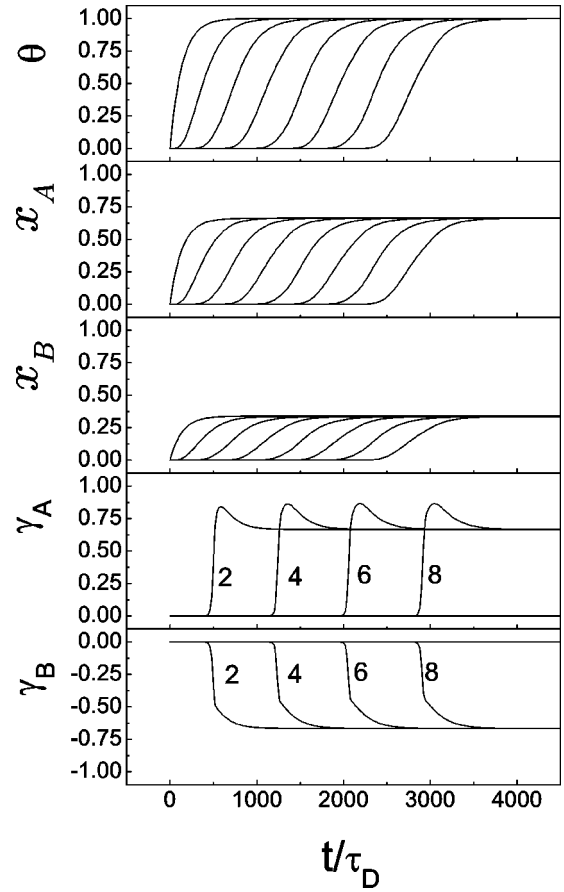


FIG. 9. The evolution of the coverage, the concentrations, and the order parameters during the growth process with  $w_A = 0.01$ ,  $w_B = 0.005$ ,  $\nu_{AV} = \nu_{BV} = 2.0$ ,  $k_B T/J = 0.1$ ,  $U_0/J = 1.0$ ,  $\mu_A = \mu_B = 0.025$  eV, and substrate with  $P_A^\alpha = P_A^\beta = 1$ .

currence of the oscillatory ordered phase will increase with the decrease to  $\kappa$ . For the different systems, those with the larger barrier energy need smaller  $\kappa$  to obtain the oscillatory ordered phase in the growth process. As shown in Fig. 5, when the barrier energy is small, the growth phase is closer to the equilibrium state and the equilibrium ordered phase is formed at moderate temperature. When the barrier energy is large, the growth phase deviates more with the equilibrium phase and kinetically induced oscillatory ordered phase occurs. When the barrier energy reaches a critical point of 1.14, the section of  $D$  and the section of  $FD$  are annexed.

Now we give an analysis on the formation process of the kinetically induced ordering oscillation. The formation of the ordering structure depends on the ratio of the atomic diffusion rate and the atomic adsorption rate. The atomic diffusion rate is affected by the growth parameters such as temperature, the barrier energy, and the characteristic exchange rate. It is also affected by the structure of the underlayer, which varies with the epitaxial multilayer growth. Thus even when we keep the growth parameters constant, the atomic diffusion rate is different among the layers. The bond broken factor  $W_{ij}$  in the atomic diffusion rate depends on the underlayer structure. Figure 6 shows the effect of the underlayer structure on the bond broken factor  $W_{AV}$  (only the part rel-

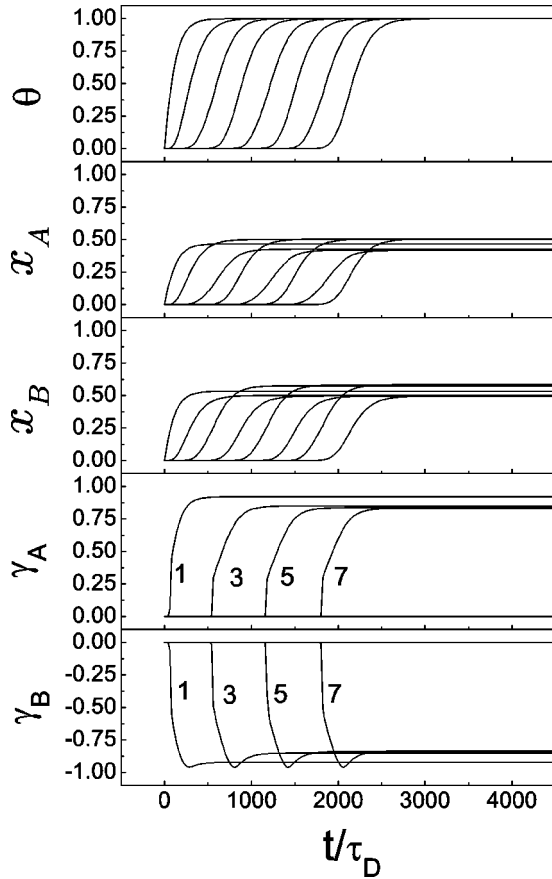


FIG. 10. The evolution of the coverage, the concentrations, and the order parameters during the growth process with  $\mu_A = -0.02$  eV,  $\mu_B = -0.01$  eV,  $k_B T/J = 0.06$ ,  $U_0/J = 1.0$ ,  $\kappa = 5 \times 10^{-3}$ , and substrate with  $P_A^\alpha = P_A^\beta = 0.5$ .

evant to the underlayer structure is shown) for atom A and vacancy exchange at temperature  $k_B T/J = 0.1$ . The bond broken factor  $W_{AV}$  has the maximum at  $P_A^\alpha = P_A^\beta = 0.5$  (disordered state). But when one of the sublattices is fully filled with one species ( $P_i^\alpha = 0$  or 1),  $W_{AV}$  reaches the minimum. For the case of Fig. 1(b), the substrate is with  $P_A^\alpha = P_A^\beta = 0.5$  initially. The atomic diffusion rate in the first layer is large, then in the first layer the ordered structure will form (e.g.,  $P_A^\alpha = 1, P_A^\beta = 0$ ). Then the atomic diffusion rate in the second layer is low and the disordered structure will form in the second layer (again  $P_A^\alpha = P_A^\beta = 0.5$ ). In such a way, it leads to the ordering oscillation with the ordered odd layers as shown in Fig. 2(b). When the substrate is initially with pure A species, the similar growth process leads to the ordering oscillation. But in this case, the even layers are ordered as shown in Fig. 2(a). When the substrate is between these two extreme cases, such as the substrate with  $P_A^\alpha = P_A^\beta = 0.25$ , the ordering oscillation will have less favorable conditions to occur.

### B. Effect of the next-nearest-neighbor interaction

We consider the cases of  $E_{AB}^{(2)} \neq 0$ . The interchange energy between the  $i$ th nearest neighbor atoms is defined as  $J^{(i)}$

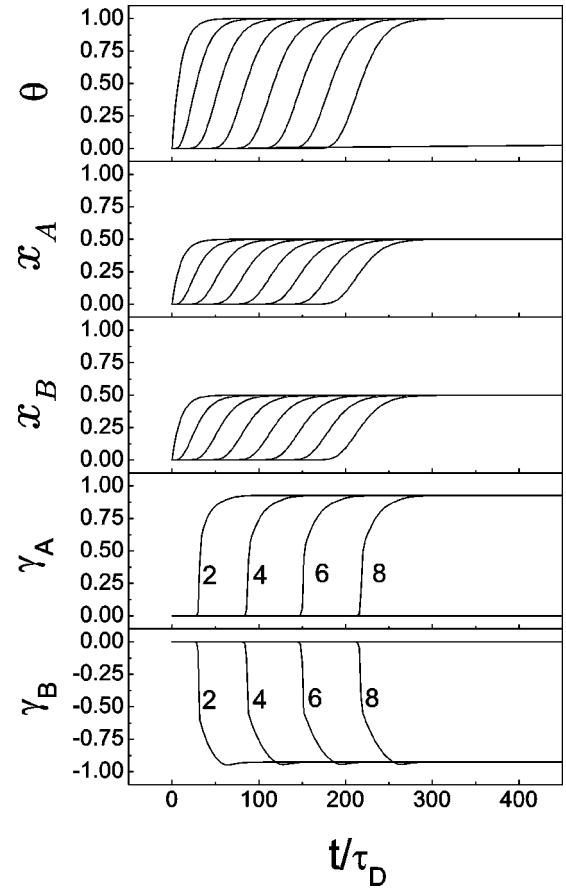


FIG. 11. The evolution of the coverage, the concentrations, and the order parameters during the growth process with  $\nu_{AV} = 0.2$ ,  $\nu_{BV} = 200.0$ ,  $w_A = w_B = 0.01$ ,  $k_B T/J = 0.06$ ,  $U_0/J = 1.0$ ,  $\mu_A = \mu_B = 0.025$  eV, and substrate with  $P_A^\alpha = P_A^\beta = 1$ .

$= -2E_{AB}^{(i)} + E_{AA}^{(i)} + E_{BB}^{(i)}$ . The next-nearest-neighbor interaction  $J^{(2)} \neq 0$  with  $E_{AB}^{(2)} \neq 0$ ,  $E_{AA}^{(2)} = E_{BB}^{(2)} = 0$ . Figure 7 shows the effect of the next-nearest-neighbor interaction  $J^{(2)}$  on the structure of the system. When  $J^{(2)}/J^{(1)} > 0.4$  the system is in disordered phase. When  $-0.29 < J^{(2)}/J^{(1)} < 0.4$ , the system forms oscillatory ordered phase at lower temperature. When  $J^{(2)}/J^{(1)} < -0.29$  the system forms ordered phase at  $k_B T/J > 0.04$ . When  $J^{(2)}/J^{(1)} > 0$ , the system tends to be in disordered phase, and when  $J^{(2)}/J^{(1)} < 0$ , the system tends to form ordered phase. The maximal temperature range of the oscillatory ordered phase is at  $J^{(2)}/J^{(1)} = -0.06$ . The second-nearest-neighbor interaction tends to reduce the temperature range of the oscillatory ordered phase. The oscillatory ordered phase might occur in the alloy systems with small ratio of the nearest- and the next-nearest-neighbor interchange energy  $J^{(2)}/J^{(1)}$  such as CuAu (Ref. 27) and NiAl (Ref. 28) alloys. The ratio between the nearest- and the next-nearest-neighbor interchange energies  $J^{(2)}/J^{(1)}$  is  $-0.2$  for CuAu alloy (Ref. 27) and  $-0.12$  for NiAl alloy (Ref. 28), which is in the range of the ratio  $J^{(2)}/J^{(1)}$  for the occurrence of the oscillatory ordered phase. Thus the oscillatory ordered phase might occur with the suitable value of the  $\kappa$  in the growth of the CuAu and NiAl alloys.

### C. Effect of the $E_{AA}^{(1)} \neq E_{BB}^{(1)}$

Now we consider the cases of  $E_{AA}^{(1)} \neq E_{BB}^{(1)}$ . When we take  $E_{AA}^{(1)} = 0.001$  eV and  $E_{BB}^{(1)} = 0.01$  eV, the order parameters are shown in Fig. 8. For showing more detail, we only show the first 8 layers of the 32 layers in Figs. 8–11. The concentration of *A* atoms is higher than that of *B* atoms in the even layers but the concentration of two species is nearly equal in the odd layers. There are small transient peaks in the curves of  $\gamma_A$ . The evaporation is proportional to the bond broken factor. We have shown that the bond broken factor depends on the underlayer structure. The bond broken factor  $V_A^\alpha$  at  $P_A^\alpha = P_A^\beta = 0.5$  (disordered state) is far bigger than that at  $P_A^\alpha = 1, P_A^\beta = 0$  (ordered state). Because of the difference between  $E_{AA}^{(1)}$  and  $E_{BB}^{(1)}$ , the bond broken factors  $V_A^\alpha$  and  $V_B^\alpha$  are different. Thus the evaporation of atom *B* is far greater than that of atom *A* when the underlayer is disordered. For the case of Fig. 8, the concentrations of two atoms are different because of  $E_{AA}^{(1)} \neq E_{BB}^{(1)}$  in the even layers, which leads to the peaks in the curves of  $\gamma_A$ .

### D. Effect of the characteristic adsorption rate

We have discussed the case of  $w_A = w_B$  above, now we discuss the case of  $w_A \neq w_B$ . When we take  $w_A = 0.01$ ,  $w_B = w_A/2 = 0.005$ , and  $k_B T/J = 0.1$ , the system has kinetically induced oscillatory ordered phase as shown in Fig. 9. We find  $x_B/x_A \approx w_B/w_A$ , which means the concentration is decided by the characteristic adsorption rate. There are peaks in the curves of the order parameter as shown in Fig. 9. They are caused by the difference between  $w_A$  and  $w_B$ . When  $w_B > w_A$ , the peaks appear in the curves of  $\gamma_B$ , and when  $w_A > w_B$ , the peaks appear in the curves of  $\gamma_A$ . When the characteristic adsorption rate of one species is bigger, they will occur one sublattice firstly, which leads to the peaks in the curves of the order parameter.

### E. Effect of the chemical potential

We consider the cases of  $\mu_A \neq \mu_B$ . When we take  $\mu_A = -0.02$  eV and  $\mu_B = -0.01$  eV, the order parameters of the system are shown in Fig. 10. When  $k_B T/J = 0.05$ , the concentration of *A* atoms is lower than that of *B* atoms in the odd layers but the concentration of two species is nearly equal in the even layers. There are peaks in the curves of  $\gamma_B$ . Similar to the effect of  $E_{AA}^{(1)}$  and  $E_{BB}^{(1)}$ , the evaporation rates are different when  $\mu_A \neq \mu_B$ . For the case of Fig. 10, the substrate is with  $P_A^\alpha = P_A^\beta = 0.5$  initially. The evaporation rate in the first layer is large and the first layer forms the ordered structure ( $P_A^\alpha = 1, P_A^\beta = 0$ ). Then the evaporation rate in the second layer is low and the second layer forms the disordered structure ( $P_A^\alpha = P_A^\beta = 0.5$ ). The concentrations of two atoms are different because  $\mu_A \neq \mu_B$  in the odd layers, which leads to the peaks in the curves of  $\gamma_B$ .

### F. Effect of the characteristic exchange rate and the barrier energy

We have discussed the case of  $\nu_{AV} = \nu_{BV}$  above, now we discuss the case of  $\nu_{AV} \neq \nu_{BV}$ . When we take  $\nu_{AV} = 0.2$ ,  $\nu_{BV} = 10^3 \times \nu_{AV} = 200$ , and  $k_B T/J = 0.06$ , the system has a kinetically induced oscillatory ordered phase as shown in Fig. 11. There are small peaks in the curves of the order parameter as shown in Fig. 11. They are caused by the difference between  $\nu_{AV}$  and  $\nu_{BV}$ . When  $\nu_{BV} > \nu_{AV}$ , the peaks appear in the curves of  $\gamma_B$ . When the characteristic exchange rate of one species is big, the system will reach the ordered phase quickly by the exchange of atoms and lead to the peak of order parameter. The basic exchange probability function  $Y_{ij}(m)$  is proportional to the barrier energy factor  $\exp(-U_{ij}/k_B T)$ . The exchange rate of the two species is also different when  $U_{AV} \neq U_{BV}$ . The results for  $U_{AV} \neq U_{BV}$  are similar to Fig. 11. The difference of the barrier energies also leads to the peaks in the curves of the order parameter.

## IV. SUMMARY

In summary, we have investigated the epitaxial growth process for a fcc alloy system. We have calculated the kinetic phase diagrams of epitaxial growth. The structure formed during the growth process depends on the growth parameters such as growth temperature, barrier energy, and the ratio of characteristic adsorption rate and atomic exchange rate. At low temperature, the frozen-in disordered phase is formed due to the low exchange rate of atoms, while the entropy induced disordered phase is formed at high temperature. The ordered phase is formed at moderate temperature. We have found that there is a kinetically induced oscillatory ordered phase in addition to the equilibrium ordered phase in the kinetic phase diagrams. This oscillatory ordered phase is caused by the nonequilibrium kinetics of the growth processes. The next-nearest-neighbor interaction tends to reduce the temperature range of the oscillatory ordered phase. The difference of the characteristic adsorption rates leads to the difference of the concentrations and the peaks of the order parameters. The effects of the chemical potentials, the characteristic exchange rates, and the barrier energies are also discussed. In the real system, this oscillatory ordered phase might occur with the condition that the next-nearest-neighbor interaction is not strong as compared with the nearest-neighbor interaction such as in CuAu (Ref. 27) and NiAl (Ref. 28) alloys. It occurs with the experimental condition of the higher deposition rate.

## ACKNOWLEDGMENTS

This research was supported by National Key Program of Basic Research Development of China (Grant No. G2000067107) and the National Natural Science Foundation of China under Grant No. 10274036.

- <sup>1</sup>A. Ourmazd and J.C. Bean, Phys. Rev. Lett. **55**, 765 (1985).
- <sup>2</sup>D.E. Jesson, S.J. Pennycook, J.M. Baribeau, and D.C. Houghton, Phys. Rev. Lett. **68**, 2062 (1992).
- <sup>3</sup>F.K. LeGous, V.P. Kesan, and S.S. Iyer, Phys. Rev. Lett. **64**, 40 (1990).
- <sup>4</sup>V.P. Kesan, F.K. LeGous, and S.S. Iyer, Phys. Rev. B **46**, 1576 (1992).
- <sup>5</sup>T.S. Kuan, T.F. Kuech, W.I. Wang, and E.L. Wilkie, Phys. Rev. Lett. **54**, 201 (1985).
- <sup>6</sup>G.B. Stringfellow and G.S. Chen, J. Vac. Sci. Technol. B **9**, 2182 (1991).
- <sup>7</sup>D. Korakakis, K.F. Ludwig, and T.D. Moustakas, Appl. Phys. Lett. **71**, 72 (1997).
- <sup>8</sup>A. Zunger and S. Mahajan, in *Handbook on Semiconductors*, edited by T. S. Moss and S. Mahajan (Elsevier, Amsterdam, 1994), Vol. 3, p. 1399.
- <sup>9</sup>B. Park, G.B. Stephenson, S.M. Allen, and K.F. Ludwig, Jr., Phys. Rev. Lett. **68**, 1742 (1992).
- <sup>10</sup>J.L. Stevens and R.Q. Hwang, Phys. Rev. Lett. **74**, 2078 (1995).
- <sup>11</sup>G.L. Zhou, M.H. Yang, and C.P. Flynn, Phys. Rev. Lett. **77**, 4580 (1996).
- <sup>12</sup>G. Abadias, I. Schuster, A. Marty, and B. Gilles, Phys. Rev. B **61**, 6495 (2000).
- <sup>13</sup>R. Venkatasubramanian, J. Mater. Res. **7**, 1235 (1992).
- <sup>14</sup>J.R. Smith and A. Zangwill, Phys. Rev. Lett. **76**, 2097 (1996).
- <sup>15</sup>M. Kotrla and M. Predota, Europhys. Lett. **39**, 251 (1997).
- <sup>16</sup>Y. Shim, D.P. Landau, and S. Pal, Phys. Rev. E **58**, 7571 (1998).
- <sup>17</sup>B. Drossel and M. Kardar, Phys. Rev. Lett. **85**, 614 (2000).
- <sup>18</sup>M. Ishimaru, S. Matsumura, N. Kuwano, and K. Oki, Phys. Rev. B **51**, 9707 (1995).
- <sup>19</sup>C.S. Deo and D.J. Srolovitz, Phys. Rev. B **63**, 165411 (2001).
- <sup>20</sup>P. Weinberger, V. Drchal, L. Szunyogh, and J. Fritscher, Phys. Rev. B **49**, 13 366 (1994).
- <sup>21</sup>Y. Saito and H. Müller-Krumbhaar, J. Chem. Phys. **70**, 1078 (1979).
- <sup>22</sup>H.T. Shi and J. Ni, Phys. Rev. B **65**, 115422 (2002).
- <sup>23</sup>L.Q. Chen and J.A. Simmons, Acta Metall. Mater. **42**, 2943 (1994).
- <sup>24</sup>G.H. Gilmer and P. Bennema, J. Appl. Phys. **43**, 1347 (1972).
- <sup>25</sup>J. Ni and B.L. Gu, Phys. Rev. Lett. **79**, 3922 (1997).
- <sup>26</sup>C.K. Hu and P. Kleban, Phys. Rev. B **25**, 6760 (1982).
- <sup>27</sup>G. Gompper and D.M. Kroll, Phys. Rev. B **38**, 459 (1988).
- <sup>28</sup>P. Cenedese, A. Marty, and Y. Calvayrac, J. Phys. (France) **50**, 2193 (1989).